Download free from www.wjtcm.net

Original Article

An Integrated Study for the Utilization of Anthraquinone Compounds Extract "Heshouwu" *In vivo* and their Comparative Metabolism in Liver Microsomes Using UPLC-ESI-Q-TOF/MS^n

Sha Chen[a], Hong-Yu Ma[a], Zhe Deng[a], Jun Zhang[a], Jin-Tang Cheng[a], Chang Chen[a], An Liu[a]

[a]Key Laboratory of Beijing for Identification and Safety Evaluation of Chinese Medicine, Institute of Chinese Materia Medica, China Academy of Chinese Medical Sciences, Beijing 100700, China

Abstract

Objective: Anthraquinone (AQ), a major bioactive component of the traditional Chinese medicine HeShouWu, has widespread applications in industry and medicine. The objective of the current study is to explore the differences in the bioavailability of anthraquinones in vivo and the metabolism in liver microsomes. **Materials and Methods:** *In vivo*, we used a reliable UPLC-ESI-QqQ-MS/MS method to measure seven AQ compounds in the jugular vein plasma of rats following oral administration of HeShouWu. Furthermore, in order to quantify the bioavailability of AQs in vivo and to further understand the metabolism of these compounds, we compared the in vitro metabolism of AQ in different species with respect to metabolic profiles, the enzymes involved, and catalytic efficiency using liver microsomes from human (HLM), mouse (MLM), rat (RLM), and beagle dog (DLM). **Results:** We identified two metabolic pathways, including the hydroxylation and glucuronidation of AQ, in the liver microsomes of humans and other species using UPLC-ESI-Q-TOF. We found that substitutions on the AQ ring were crucial to the activity and regioselectivity of its hydroxylation. In general, hydroxylation activity decreased greatly with β-COOH (rhein) and enhanced dramatically with β-OH (emodin). We also found that glucuronidation of the compound emodin-8-O-β-D-glucoside acts as the main isoform in AQ hydroxylation in HLM and DLM. Total microsomal intrinsic clearance values for AQ were greatest in mouse microsomes, followed by those in dog, human, and rat microsomes. **Conclusion:** The absorption of different anthrquinone compounds varied based on the compound structure, the metabolism types and products of anthraquinones in liver microsomes were different in different species. These findings provide vital information for a deeper unuunderstanding of the metabolism of AQs.

Keywords: Anthraquinones, liver microsomes, UPLC-QqQ-MS/MS, UPLC-Q-TOF/MS

Introduction

Anthraquinones (AQs) are widely distributed in many medicinal plants and can be found in the metabolites of lower plants.[1] AQs are the main components of radix polygoni multiflori (RPM, Heshouwu in Chinese) and have many biological activities that can combat cancer[2-4] and developmental anomalies,[5] as well as tonic tension.[6] AQs also have antimicrobial,[7] antioxidant,[8] and anti-human cytomegalovirus activity.[9] Previously, AQs were primarily used in the dye industry. More recently, they have gained attention as a result of the identification of their significant medical value, and *Polygonum multiflorum* is currently employed in clinical practice.

RPM is an herb thought to tonify the kidney and liver and has also been used to treat hyperlipidemia and the premature graying of hair.[10-13] However, a growing number of studies have also demonstrated the adverse effects of *P. multiflorum*,[14-16] and some researchers found that *P. multiflorum* can cause hepatotoxicity. In addition, the long-term use of *P. multiflorum* may also lead to

Access this article online

Quick Response Code:

Website: www.wjtcm.net

DOI: 10.4103/wjtcm.wjtcm_2_18

Address for correspondence: Prof. An Liu , Key Laboratory of Beijing for Identification and Safety Evaluation of Chinese Medicine, Institute of Chinese Materia Medica, China Academy of Chinese Medical Sciences, No. 16, Nanxiaojie, Dongzhimennei, Beijing 100700, China.
E-mail: wjtcmoffice@vip.126.com

This is an open access journal, and articles are distributed under the terms of the Creative Commons Attribution-NonCommercial-ShareAlike 4.0 License, which allows others to remix, tweak, and build upon the work non-commercially, as long as appropriate credit is given and the new creations are licensed under the identical terms.

For reprints contact: reprints@medknow.com

© 2018 World Journal of Traditional Chinese Medicine | Published by Wolters Kluwer - Medknow

Received: 16-06-2017, **Accepted:** 12-03-2018

How to cite this article: Chen S, Ma HY, Deng Z, Zhang J, Cheng JT, Chen C, *et al*. An integrated study for the utilization of anthraquinone compounds extract "Heshouwu" *In vivo* and their comparative metabolism in liver microsomes using UPLC-ESI-Q-TOF/MSn. World J Tradit Chin Med 2018;4:21-7.

kidney toxicity. Such adverse effects may be induced directly by AQs present in RPM or by a reactive metabolite of the chemical constituents acting against hepatocytes.[13,15]

In this study, we analyzed the behavior of AQ *in vitro* and *in vivo* through administration of "HeShouWu" by gavage, in order to provide a basis for the study of liver toxicity. It is of great importance to investigate the metabolic behavior of AQs and to identify whether nephrotoxicity is caused by AQ components in *P. multiflorum*. The present research identifies the biotransformative role of AQs. We used liver microsomes from various species (including human, beagle, Sprague Dawley (SD) rat, and CD1 mouse) to verify bioconversion relationships and to investigate the metabolism of AQ compounds *in vitro*. Such research may in turn help the design of new drugs and enhance the use of *P. multiflorum* in clinical applications.

Experimental

Chemicals and materials

RPM (NO.201311015) was purchased from Infinitus Co. Ltd., (Beijing, China). Standard compounds of rhein (No. 0757-9804), emodin (No. 0756-9707), aloe-emodin (No. 110795-201007), chrysophanol (110796–201319), physcion (0758–9402) (>98%), and saikosaponin A (internal standard [IS]) were purchased from the National Institute for the Control of Biological and Pharmaceutical Drugs (Beijing, China). Emodin-8-O -β-D-glucoside (emodin-8-O-β-D-Glu, >97.6%) was obtained from the laboratory where the study was conducted, and proton nuclear magnetic resonance (H-NMR) and carbon NMR spectra were applied. Glucose-6-phosphate (G6P) dehydrogenase and NADP-Na_2 were purchased from Roche (Roche, Switzerland). Hydrated magnesium chloride ($MgCl_2(H_2O)_6$) was purchased from Amresco (Amresco, USA). Uridine diphosphate glucuronic acid (UDPGA) was purchased from Sigma. Alamethicin was purchased from Aladdin (Aladdin, USA). Mass spectrometry (MS)-grade acetonitrile and methanol were obtained from Sigma-Aldrich (St. Louis, MO, USA). The formic acid used (eluent additive used for high-performance liquid chromatography-MS [HPLC-MS] analysis) was also of MS grade (CNW, Germany). Other analytical-grade chemicals were obtained from the Beijing Chemical Factory (Beijing, China).

Human, beagle dog, rat, and mouse liver microsomes were purchased from XenoTech (XenoTech, USA). All liver microsomes were from adult males. All procedures involving animals complied with the Laboratory Animal Management Principles of China. Microsomes prepared from liver tissue using differential ultracentrifugation were used to determine the concentration of microsomal protein with bovine serum albumin used as a standard. All microsomal samples were stored at − 80°C until further use.

Experimental animals

Adult male SD rats weighing 200 ± 20 g were examined by the National Institute for Food and Drug Control (Beijing, China; Certificate No. SCXK2009-0017). The animals were specifically pathogen-free, had been acclimated to their environmentally controlled quarters for at least three months (24°C ± 1°C, 12/12 h light/dark cycles), and had free access to standard food and water.

Blank plasma was collected before the experiment. All experimental protocols were conducted in accordance with the Guide for the Care and Use of Laboratory Animals (National Institute of Health Publication 85–23, revised edition 1985).

Preparation of radix polygoni multiflori extract

RPM samples were weighed accurately (70 g) and placed into a conical flask. The soluble constituents were extracted by refluxing in 70% alcohol three times, first for 90 min, then for 70 min, and finally for 50 min. The extracts were combined and concentrated under vacuum, then diluted with water to 50 mL. A single dose of "Heshouwu" equivalent to 21 g/kg of crude drugs was administered to rats.

Preparation of plasma samples

Plasma samples were collected from the jugular vein. Plasma was collected at 0 min, 5 min, 10 min, 15 min, 20 min, 30 min, 45 min, 1 h, 2 h, 4 h, 8 h, 12 h, and 24 h after intragastric administration of the extract using an online automatic blood collection operation. Approximately 250 μL of blood was placed in Eppendorf tubes (EP tubes) containing heparin sodium. These were mixed immediately and centrifuged at 4000 × g for 10 min. The plasma samples were then transferred to new 1.5-mL EP tubes and stored at −20°C until further use.

The 100-μL plasma samples were placed in a tube containing IS and vortexed for 1 min, after which 400 μL acetonitrile was added to precipitate proteins. The mixture was vortexed for 2 min and centrifuged at 12 000 × g for 5 min. The 400-μL supernatant was then transferred to another 5-mL EP tube and evaporated to dryness under a stream of nitrogen at 25°C. The residue was dissolved in 150 mL methanol-water solution (50/50, v/v) and centrifuged at 12000 × g for 5 min. The supernatant was then transferred to another EP tube and filtered through a 0.22-μm Millipore filter before HPLC-MS analysis.

Pharmacokinetics

The pharmacokinetic parameters of maximum plasma concentration (C_{max}) and the time of maximum plasma concentration (T_{max}) were measured directly from the plasma data. The elimination rate constant (*Ke)* was evaluated using linear regression of the terminal points in a semi-log plot of plasma concentration against time. Elimination half-life ($t_{1/2}$) was calculated using the formula $t_{1/2} = 0.693/K_e$. The area under the plasma concentration time curve from time zero to infinity ($AUC_{0-\infty}$) was calculated as $AUC_{0-\infty} = AUC_0 - T_{0-t} + C_t/K_e$.

Liver microsomal incubation

Preparation of substrate

Emodin-8-O-β-D-Glu, physcion-8-O-β-D-glucoside, aloe-emodin, rhein, emodin, chrysophanol, and physcion

were dissolved in dimethyl sulfoxide (DMSO) to obtain concentrations of 12.75, 11.89, 15.00, 11.51, 11.50, 11.07, and 14.61 mM, respectively.

Preparation of phase I metabolite solutions

NADPH-Na_2 was prepared as a 10 mM solution in phosphate buffer. Both G6P and $MgCl_2$ were prepared as 50 mM solutions in phosphate buffer. G6PD was dissolved in phosphate buffer to achieve a concentration of 10 units/mL. All samples were aliquoted and stored at −20°C until further use.

Preparation of phase II metabolite solutions

$MgCl_2$ was prepared as an 8 mM solution in phosphate buffer, alamethicin was prepared as a 125 μg/mL solution in phosphate buffer, and UDPGA was prepared as a 5 mM solution in phosphate buffer. All were stored as aliquots at −20°C until further use.

Liver microsomal incubation for phase I metabolites

Complete incubation systems contained 2 μL AQ compounds, 78 μL phosphate buffer, 40 μL G6P dehydrogenase, and 40 μL SD rat liver microsomes. The mixture was preincubated for 5 min and then added to 40 μL cofactor solution, which was also preincubated for 5 min. The reaction was initiated by further incubating for 1 h at 37°C. The mixture was then centrifuged at 4000 × g, and the reaction was terminated by adding 200 μL ice-cold methanol. The mixture was maintained at − 20°C for 10 min, vortexed for 2 min, and then centrifuged at 10000 × g for 5 min. The supernatant was drawn into another tube and dried with a gentle stream of nitrogen gas. The residue was dissolved in 150 μL methanol, then vortexed, and centrifuged as described above. Reactions for all other liver microsomes (human, beagle, and CD1 mouse) were conducted in the same manner.

Liver microsomal incubation for phase II metabolites

Incubation systems for phase II metabolites were different from those of phase I metabolites. Incubation solutions contained 2 μL AQ compounds, 38 μL phosphate buffer, 40 μL $MgCl_2$ solution, 40 μL alamethicin solution, and 40 μL SD rat liver microsomes. The mixture was preincubated for 5 min, and then added to 40 μL UDPGA, which was also preincubated for 5 min. The remaining procedure was performed as described above. Reactions for all other liver microsomes (human, beagle, and CD1 mouse) were conducted in the same manner.

Chromatographic system

An HPLC-20A unit, equipped with a photodiode array detector, was used to analyze the reference and AQ compounds extracted from RPM. An Agilent Eclipse Plus C_{18} (50 mm × 2.1 mm, 1.8 μm) analytical column was used for this analysis.

The mobile phase consisted of methanol (A) and water containing 0.2% (v/v) formic acid (B) with the following gradient profile: 0–1.5 min, 10% A; 1.5–1.6 min, increase to 70% A; 1.6–3.6 min, 70% A; 3.6–3.7 min, increase to 80% A; 3.7–8.0 min, 80% A; 8–13 min, 95% A. The flow rate was 0.2 mL/min, column temperature was maintained at 35°C, and the injection volume was 3 μL.

To study the metabolites of AQ compounds *in vitro*, an agilent eclipse plus C_{18} (100 mm × 3 mm, 1.8 μm) analytical column was used. The mobile phases comprised acetonitrile as solvent A and MS-grade water containing 0.1% (v/v) formic acid as solvent B. The following gradient profile was used: 0–1.5 min, 10% A; 1.5–4 min, increase to 50% A; 4–10 min, increase to 95% A; 10–13 min, 95% A; at a flow rate of 0.8 mL/min and a column temperature of 35°C. The injection volume was 5 μL, and the diode array detection wavelength for data acquisition was set to 254 nm.

Quantitative detection was carried out using UPLC-ESI -QqQ-MS (Agilent 1290 and 6460 triple quadrupole MS series, Agilent Corporation, CA, USA). Electrospray ionization (ESI) was performed in negative mode. The mass spectrometric parameters for each compound (tetrahydroxystilbene glucoside [TSG], rhein, emodin-8-O-β-Glu, aloe-emodin, emodin, chrysophanol, and 1, 8-didroxyanthraquinone) were all optimized in our study.

Qualitative analyses of various liver microsomes were carried out using UPLC-Q-TOF/MS. ESI was also performed in negative mode, with nitrogen used as the drying agent in MS analysis. MS conditions were as follows: nebulizing pressure, 35 psi; gas flow, 5 L/min; gas temperature, 325°C; sheath gas flow and temperature, 12 L/min and 350°C, respectively; accelerating voltage, 175 V; and collision energy, 25 V.

Statistical analysis

The software DAS 2.0 was used to plot graphs and analyze the pharmacokinetic parameters of AQ. Metabolite data were identified through UPLC-ESI-Q-TOF-MS after incubating mono-AQs with various liver microsomes.

Results

Optimization of UPLC-ESI-QqQ-MS^n

To take advantage of the high sensitivity of multiple reaction monitoring (MRM) in the quantitative analysis, standards were used to generate characteristic $MS^{[2]}$ ions for quantification. We optimized representative MRM chromatograms of the IS (1,8-didroxyanthraquinone) and analytes (TSG, emodin, emodin-8-O-β-D-Glu, aloe-emodin, rhein, and chrysophanol) extracted from rat plasma samples following oral administration of the Heshouwu extract [Figure 1]. For TSG, emodin, emodin-8-O-β-D-Glu, aloe-emodin, rhein, and chrysophanol, the optimized suitable paired ions ($[M-H]^-$MS/MS $[Q3]^-$) were 405.1–243, 269.1–241, 431.1–269.1, 269.1–239.1, 283.1–239.1, and 253.1–225.1, respectively. Other ion pairs ($[M-H]^-$[Q3]$^-$) were used for qualitative and quantitative analysis. These were 405.1–225, 269.1–225.1, 431.1–25.1, 269.1–211, 269.1–225.1, and 253.1–182, respectively [Table 1].

Method validation

Calibration curves

Calibration curves were constructed by plotting the peak area ratio of the analyte to the IS against the nominal concentration of the analyte. Calibration curve parameters and limits of detection for

AQs are shown in Table 2. The correlation coefficient r^2 was 0.9985 for TSG, 0.9812 for emodin, 0.9995 for emodin-8-O-β-D-Glu, 0.9993 for aloe-emodin, 0.9910 for rhein, 0.9812 for emodin, and 0.9952 for chrysophanol. These data showed that all AQs exhibited relatively good linearity ($r^2 > 0.99$).

Recovery, precision, and stability

Recovery, determined from six replicates at three different concentration levels, was 87.16%–118.81% [Table 3] and within the acceptable range of values. The precision of the proposed method was assessed based on repeatability (intraday analysis, $n = 3$) and intermediate precision (interday analysis, $n = 6$) for the standards. The relative standard deviations (RSDs) for the six compounds did not exceed 19%, indicating a good level of reproducibility. Sample stability was assessed based on short-term and freeze-thaw stability. The six AQs were stable under both conditions. The RSDs were 2.17%–13.23% and 7.67%–35.85% [Table 3] for short-term and freeze-term conditions, respectively. These findings indicate that the sample solutions were stable under both freezing and warm conditions for a relatively long time (24 h).

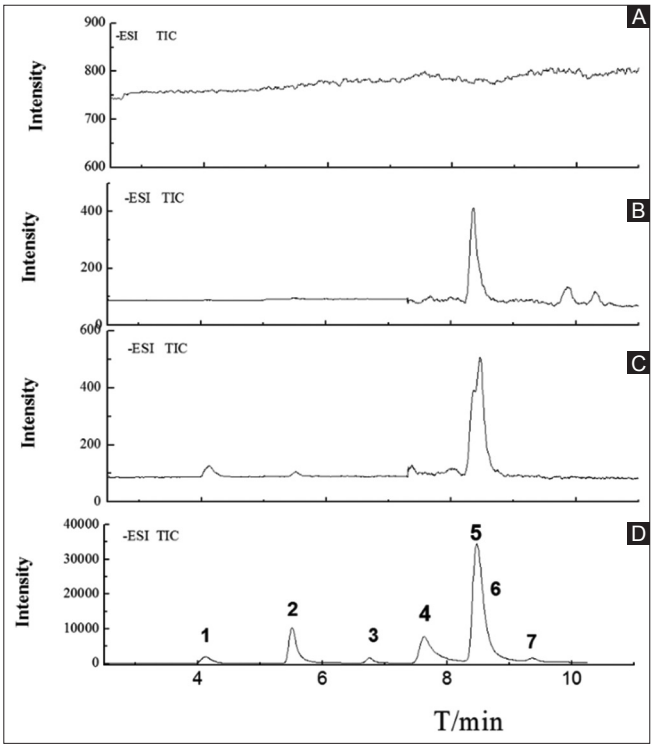

Figure 1: The multiple reaction monitoring chromatograph of standard anthraquinones and IS in blank plasma and sample plasma (A: Blank plasma, B: Blank plasma and IS, C: Sample, D: QC sample,). The peak number in D 1: TSG, 2: Emodin-8-o-β-D-glucoside, 3: Aloe-emodin, 4: Rhein, 5: IS, 6: Emodin,7: Chrysophanol

Application to pharmacokinetic studies

The optimized UPLC-QqQ-MS/MS method was successfully applied to a pharmacokinetic study measuring AQs in SD rat plasma following oral administration of high and low doses of RPM. In our study, three AQ compounds were detected after oral administration of the RPM extract. These included TSG, emodin, and emodin-8-O-β-D-Glu. We found that these three AQ compounds were rapidly absorbed in SD rat plasma as T_{max} was reached after no longer than 2.46 h for any of the three compounds [Table 4]. On the other hand, AQs were no longer detectable at 3 h after oral administration, suggesting that the compound is rapidly eliminated from SD rat plasma. The mean $AUC_{(0-\infty)}$ values did not exceed 12.35 ng/mL · h, indicating that AQ compounds have relatively low bioavailability.

Our comparison of high and low doses of RPM extract revealed that the metabolic parameters of TSG administered at both doses were very similar. This finding indicates that TSG may become saturated even at a low dosage. With regard to emodin and emodin-8-O-β-D-Glu, the high dosage produced higher C_{max} and AUC values that the low dosage. According to previous reports, in clinical contexts, large dosages of RPM can damage the liver, but such damage occurs randomly among individuals. Our results suggest that there may be multiple components of Chinese herbal medicine that can affect absorption and utilization.

Hydroxylated metabolic pathway of anthraquinones in liver microsomes

To elucidate the absolute structure and metabolic labile sites of AQ in HLM, MLM, RLM, and DLM, monohydroxylated metabolites of AQ were biosynthesized and characterized using UPLC-ESI-Q-TOF. No rhein metabolites were detected in any of the microsomes. This finding validates the theory that if the compound contains β-COOH, constitution may influence hydroxylation. Of greater importance, the major products biotransformed by this strain were characterized using UPLC-ESI-Q-TOF. These were found to have identical

Table 1: Ion pairs for multiple reaction monitoring scanning and turbo spray source for monitoring anthraquinones and the internal standard

Compounds	Precursor ion	Fragmentor (V)	Product ion (1)	CE1 (V)	Production (2)	CE2 (V)	Dwell (ms)
TSG	405.1	150	243	10	225	20	30
Rhein	283.1	60	239.2	10	183	10	20
Emodin-8-O-β-D-glu	431.1	230	269.1	20	225.1	30	40
Aloe-emodin	269.1	200	239.1	10	211	30	30
Emodin	269.1	180	241	10	225.1	10	30
Chrysophanol	253.1	230	225.1	10	182	20	20
1,8-didroxyanthraquinone	239.1	210	211.1	10	167	20	30

TSG: Tetrahydroxystilbene glucoside, CE: Collision energy

Table 2: Calibration curve parameters and limits of detection for anthraquinones

Compounds	Regression equation	Linear range (ng/mL)	r^2	LOQ (ng/mL)
TSG	y=1.3118x+0.2599	13.40-16,080	0.9985	13.4
Emodin	y=11.9223x+0.1609	2.92-1750	0.9812	2.92
Emodin-8-O-β-D-glu	y=4.5121x+0.1778	4.32-5180	0.9995	4.32
Aloe-emodin	y=0.1980x+0.0208	5.77-6920	0.9993	5.77
Rhein	y=0.6382x+0.1631	8.70-10,440	0.9910	8.70
Chrysophanol	y=0.3709x+0.0467	5.03-3020	0.9952	5.03

LOQ: Limit of quantitation, TSG: Tetrahydroxystilbene glucoside

Table 3: Mean extraction recovery and matrix effect of anthraquinones (mean±standard deviation, percentage), intra- and inter-precision, stability (short-term and freeze-thaw) of tetrahydroxystilbene glucoside, emidin-8-O-β-D-glu, aloe-emodin, rhein, emodin, chrysophanol of the Heshouwu extract

Characteristic indexes	Concentration	Compounds					
		TSG (%)	Emodin-8-O-β-D-glu (%)	Aloe-emodin (%)	Rhein (%)	Emodin (%)	Chrysophanol (%)
Recovery (*n*=6)	High	87.86±8.27	96.60±2.14	107.82±7.60	94.69±3.72	119.01±2.39	108.73±4.15
	Middle	105.84±1.04	99.53±1.80	116.14±0.39	87.16±11.66	113.26±1.21	95.86±0.59
	Low	101.45±4.61	105.18±1.43	110.45±2.34	87.21±7.13	118.81±4.24	100.56±1.25
Matrix effect (*n*=6)	High	62.89±1.61	86.47±0.85	87.16±0.60	87.08±0.55	105.06±1.23	71.12±1.07
	Middle	73.87±0.21	98.00±0.70	98.78±1.51	96.75±0.89	122.90±0.80	68.11±1.49
	Low	77.74±0.35	82.09±0.74	96.33±2.43	87.58±2.14	136.36±3.31	95.87±0.57
Precision							
Intra-precision (*n*=6)	High	8.85	7.47	8.06	7.13	7.78	8.19
	Middle	6.09	4.99	4.44	4.99	3.67	4.14
	Low	18.45	5.98	10.04	11.08	9.18	7.65
Inter-precision (*n*=3)	High	13.47	6.74	10.87	10.94	4.01	7.79
	Middle	4.81	8.25	7.75	14.67	9.65	4.97
	Low	7.49	3.89	3.49	5.59	2.35	3.69
Stability							
Short-term (*n*=3)	High	2.93	2.17	2.65	4.09	3.26	3.54
	Middle	3.55	5.66	5.04	2.99	6.63	6.06
	Low	5.71	6.18	8.23	6.47	13.23	8.96
Freeze-thaw (*n*=3)	High	19.43	7.67	8.68	16.07	11.04	-
	Middle	32.27	15.27	16.86	15.99	13.91	-
	Low	35.85	19.38	29.91	16.95	22.06	-

TSG: Tetrahydroxystilbene glucoside

retention times, UV spectra, and mass spectra to those of metabolites formed during incubation in the various liver microsomes. In addition, the substituent of the parent ring significantly impacted the hydroxylation reaction. Activity decreased greatly in the presence of β-COOH and increased dramatically in the presence of β-OH. Thus, the positional preference for hydroxylation of AQs follows this descending order: β-OH > β-CH_2OH > β-COOH [Figure 2]. The β-OH oxidation pathway prevailed in the same way among liver microsomes from the different species. This finding indicates that the hydroxylated metabolic pathway of AQs in liver microsomes may have no relation to the species.

Glucuronidation metabolic pathway in liver microsomes

Glucuronidation, another metabolism reaction, was catalyzed using UDP-glucuronosyltransferases, which are generally highly expressed in liver microsomes. The glucuronidation of six AQs in microsomes from rats, mice, humans, and dogs was characterized *in vitro*. The glucuronidation activity of each AQ was not only decided by the kind of substrate but was also related to the number of hydroxyl groups on the substrate.

Emodin and aloe-emodin have three different kinds of metabolites. The presence of emodin-8-O-β-D-Glu, although low, was supported by the observation that its monoglucuronide formed in the four microsomes. In the present study, β-alcoholic OH (aloe-emodin) glucuronidation only occurred at an −OH group. We observed slight regioselectivity of the AQs in glucuronidation at -OH, and in particular at C-8-OH, in the presence of β-CH_3 (chrysophanol), and β-OCH_3 and β-CH_3 (physcion) substituents.

Previous studies have shown that it is difficult to address the influence of β-COOH (rhein) on the regioselectivity of the glucuronidation of AQs. Similarly, in the present study, no metabolites were detected, perhaps because of the structures that were formed by glucuronidation. It is worth noting that

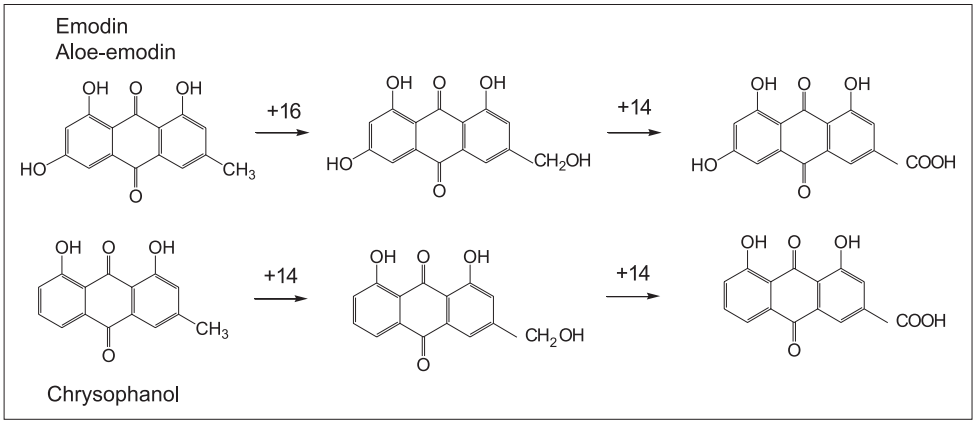

Figure 2: Pathway for oxidation of β-CH3 among anthraquinone compounds.

Table 4: Mean pharmacokinetic parameters of anthraquinones after oral administration of radix polygoni multiflori (mean±standard deviation, *n*=8)

Detected compounds	Parameter	Unit	Radix polygoni multiflori	
			Low	High
TSG	C_{max}	mg/L	0.87±0.54	0.90±0.64
	T_{max}	h	0.25±0.08	0.30±0.07
	$AUC_{0-\infty}$	mg/L·h	0.62±0.45	0.78±0.45
	$t_{1/2}$	h	1.01±0.93	0.74±0.34
	$MRT_{0-\infty}$	h	1.51±1.17	1.15±0.43
Emodin-8-O-β-D-glu	C_{max}	mg/L	0.10±0.06	0.48±0.30
	T_{max}	h	0.40±0.23	0.42±0.22
	$AUC_{0-\infty}$	mg/L·h	0.08±0.03	0.21±0.24
	$t_{1/2}$	h	1.25±0.58	1.02±0.46
	$MRT_{0-\infty}$	h	1.82±0.76	1.72±0.73
Emodin	C_{max}	mg/L	0.02±0.01	0.10±0.08
	T_{max}	h	0.17±0.00	2.46±3.99
	$AUC_{0-\infty}$	mg/L·h	0.20±0.08	0.42±0.17
	$t_{1/2}$	h	7.85±3.93	7.53±5.19
	$MRT_{0-\infty}$	h	16.04±4.49	13.00±5.51

$AUC_{0-\infty}$: Area under the plasma concentration-time curve from time zero to infinity, C_{max}: Maximum plasma concentration, T_{max}: Time of maximum plasma concentration, $t_{1/2}$: Elimination half-life, TSG: Tetrahydroxystilbene glucoside, $MRT_{0-\infty}$: Mean residence time

in addition to substrate structure, there were also differences between species and contributions to species' differences in the glucuronidation of AQ observed in the microsome-based assay *in vivo*.

AQs were not only metabolized in different ways and through different pathways but were also transformed into different metabolites. There were qualitative and quantitative differences in metabolism between emodin-8-O-β-D-Glu and rhein compounds. Our results revealed that emodin-8-O-β-D-Glu had two hydroxylated compounds in DLM and only one monohydroxylated compound in RLM, MLM, and HLM. Physcion-8-O-β-D-glucoside was only detected in metabolites in the HLM system, while no compound was detected in the other three systems. The other five AQs had no disparate variability between species.

Discussion and Conclusion

We used UPLC-QqQ-MS/MS to quantitatively analyze AQ compounds *in vivo* after oral administration of *P. multiflorum* in rats. The concentration ratio of each AQ in *P. multiflorum* was different *in vitro* compared to that *in vivo*. Thus, it can be concluded that in RPM, AQs may not be transferred *in vitro*.

In this study, we combined *in vivo* bioavailability analysis and *in vitro* liver microsome metabolism analysis to investigate six AQ compounds. The different compounds had characteristic absorption and elimination rates. The structure of rhein, aloe-emodin, and chrysophanol differed, with varying substitutions at β-positions (C-3). They were substituted with–COOH,–CH_2OH, and–CH_3, respectively. We found that chrysophanol could be oxidized to aloe-emodin and that aloe-emodin could be oxidized to rhein *in vivo*. These findings suggest that rhein may be transformed by chrysophanol and aloe-emodin through phase I metabolism. The putative conclusion from the bioavailability analysis was also validated through investigations involving liver microsomes.

Metabolism pathways leading to specific compounds may be deduced by the metabolic differences between the different species. There has not yet been detailed analysis and comparison of a number of liver microsomes. We identified two pathways, glucuronidation and hydroxylation, involved in the metabolism of AQ in RLM, whereas species-specific deacetylation of AQ has previously been well characterized as an important metabolic pathway.

A large amount of rhein was detected *in vivo*. In order to explore the metabolic pathways, we employed liver microsome incubation to analyze metabolites *in vitro*. We found that rhein had no corresponding metabolites, and the substance was absorbed and eliminated as the parent compound. This result is consistent with those of previous studies, which have found that rhein is metabolized in the kidney unchanged. We also found evidence that aloe-emodin and chrysophanol can be transformed into rhein by oxidase during phase I metabolism.

Conclusion

The absorption of different anthrquinone compounds varied based on the compound structure, the metabolism types and products of anthraquinones in liver microsomes were different in different species. These findings provide vital information for a deeper understanding of the metabolism of AQs.

Acknowledgments

We are grateful for financial support from the Major Scientific and Technological Special Project for ''Significant New Drugs Creation'' (No. 2014ZX09304307).

Financial support and sponsorship

We are grateful for financial support from the Major Scientific and Technological Special Project for ''Significant New Drugs Creation'' (No. 2014ZX09304307).

Conflicts of interest

There are no conflicts of interest.

References

1. Lin L, Ni B, Lin H, Zhang M, Li X, Yin X, *et al.* Traditional usages, botany, phytochemistry, pharmacology and toxicology of *Polygonum multiflorum* thunb.: A review. J Ethnopharmacol 2015;159:158-83.
2. Ma YS, Weng SW, Lin MW, Lu CC, Chiang JH, Yang JS, *et al.* Antitumor effects of emodin on LS1034 human colon cancer cells *in vitro* and *in vivo*: Roles of apoptotic cell death and LS1034 tumor xenografts model. Food Chem Toxicol 2012;50:1271-8.
3. Lin JG, Chen GW, Li TM, Chouh ST, Tan TW, Chung JG, *et al.* Aloe-emodin induces apoptosis in T24 human bladder cancer cells through the p53 dependent apoptotic pathway. J Urol 2006;175:343-7.
4. Yu JQ, Bao W, Lei JC. Emodin regulates apoptotic pathway in human liver cancer cells. Phytother Res 2013;27:251-7.
5. Yon JM, Lin C, Oh KW, Baek HS, Lee BJ, Yun YW, *et al.* Emodin prevents ethanol-induced developmental anomalies in cultured mouse fetus through multiple activities. Birth Defects Res B Dev Reprod Toxicol 2013;98:268-75.
6. Lim KM, Kwon JH, Kim K, Noh JY, Kang S, Park JM, *et al.* Emodin inhibits tonic tension through suppressing PKCδ-mediated inhibition of myosin phosphatase in rat isolated thoracic aorta. Br J Pharmacol 2014;171:4300-10.
7. Ali AM, Ismail NH, Mackeen MM, Yazan LS, Mohamed SM, Ho AS, *et al.* Antiviral, cyototoxic and antimicrobial activities of anthraquinones isolated from the roots of *Morinda elliptica*. Pharm Biol 2000;38:298-301.
8. Yen GC, Duh PD, Chuang DY. Antioxidant activity of anthraquinones and anthrone. Food Chem 2000;70:437-41.
9. Barnard DL, Fairbairn DW, O'Neill KL, Gage TL, Sidwell RW. Anti-human cytomegalovirus activity and toxicity of sulfonated anthraquinones and anthraquinone derivatives. Antiviral Res 1995;28:317-29.
10. Wang JB, Kong WJ, Wang HJ, Zhao HP, Xiao HY, Dai CM, *et al.* Toxic effects caused by rhubarb (*Rheum palmatum* L.) are reversed on immature and aged rats. J Ethnopharmacol 2011;134:216-20.
11. Wang J, Zhao Y, Xiao X, Li H, Zhao H, Zhang P, *et al*. Assessment of the renal protection and hepatotoxicity of rhubarb extract in rats. J Ethnopharmacol 2009;124:18-25.
12. Wu X, Chen X, Huang Q, Fang D, Li G, Zhang G, *et al.* Toxicity of raw and processed roots of *Polygonum multiflorum*. Fitoterapia 2012;83:469-75.
13. Yu J, Xie J, Mao XJ, Wang MJ, Li N, Wang J, *et al.* Hepatoxicity of major constituents and extractions of radix polygoni multiflori and radix polygoni multiflori praeparata. J Ethnopharmacol 2011;137:1291-9.
14. Lin L, Lin H, Zhang M, Ni B, Yin X, Qu C, *et al.* A novel method to analyze hepatotoxic components in *Polygonum multiflorum* using ultra-performance liquid chromatography-quadrupole time-of-flight mass spectrometry. J Hazard Mater 2015;299:249-59.
15. Lv GP, Meng LZ, Han DQ, Li HY, Zhao J, Li SP, *et al.* Effect of sample preparation on components and liver toxicity of *Polygonum multiflorum*. J Pharm Biomed Anal 2015;109:105-11.
16. Noda T, Yamada T, Ohkubo T, Omura T, Ono T, Adachi T, *et al*. Hot-water-extracts of *Polygonum multiflorum* do not induce any toxicity but elicit limited beneficial effects on the liver in mice. J Health Sci 2009;55:720-5.